Ultrafast resonant terahertz response of excitons in semiconductor quantum dots

T. Müller,[1,*] W. Parz,[1] K. Unterrainer,[1] S. Sauvage,[2] J. Houel,[2] P. Boucaud,[2] A. Miard,[3] and A. Lemaître[3]
[1]*Institut für Photonik and Zentrum für Mikro- und Nanostrukturen, TU Wien, A-1040 Wien, Austria*
[2]*Institut d' Electronique Fondamentale, CNRS, Universite Paris-Sud, F-91405 Orsay, France*
[3]*Laboratoire de Photonique et Nanostructures, CNRS, Route de Nozay, F-91460 Marcoussis, France*
(Received 21 November 2007; published 14 January 2008)

Exciton formation and carrier-carrier interactions in semiconductor quantum dots have been investigated by means of terahertz time-domain spectroscopy. The formation of excitons leads to a blueshift of the terahertz absorption as compared to the bare electronic intersublevel absorption. We show that this is a consequence of Coulomb interactions among carriers in the quantum dots. Time-resolved studies reveal the time scale on which photogenerated electron-hole pairs in the GaAs barriers transform into confined excitons in the dots.

DOI: 10.1103/PhysRevB.77.035314 PACS number(s): 78.67.Hc, 71.35.−y, 73.21.La, 78.47.−p

Coulomb interaction between electrical charges is one of the most fundamental phenomena in nature. Quantum dots (QDs) form an ideal model system to explore Coulomb interactions in solids, because they allow studying interactions between a small, countable number of charged particles. The past two decades have therefore seen considerable experimental and theoretical efforts to gain insight in the details of few-particle interactions in QDs.[1] The vast majority of research has focused on interband optical studies, whereas intersublevel (ISL) transitions,[2–4] which occur in the mid- or far infrared (FIR), have received comparably little attention. One reason might be that this frequency regime is one of the least technologically developed ranges in the electromagnetic spectrum. Another, more fundamental, reason is that ISL studies are traditionally performed on doped samples, i.e., involve only one type of carrier, and hence are rather insensitive to many-particle effects.[5,6] If electrons and holes are present, however, the FIR radiation couples differently to both types of carriers and the absorption can strongly deviate from that of a single particle.[7] This opens new opportunities for FIR spectroscopy of few-particle states in zero-dimensional systems. Interband optical studies are based on the creation and/or destruction of electron-hole *pairs*, and are thus *per se* not capable of probing the single-particle excitations of a system. In contrast, ISL spectroscopy can provide information on both single- *and* many-particle properties and hence allows for a quantitative determination of the strength of Coulomb interactions in QDs.

Employing optical-pump and terahertz-probe spectroscopy, we have studied Coulomb interactions in zero-dimensional systems by examining the behavior and dynamics of photogenerated excitons in *n*-doped InAs QDs. In contrast to previous terahertz time-domain studies of QDs,[8,9] where the terahertz photon energy was smaller than any energy level spacing in the QDs, the absorption signals in our experiments are determined by the *resonant* response of the ISL transitions.

The sample for the present study was grown by molecular beam epitaxy and consists of 80 layers of InAs self-assembled QDs, separated by 50 nm thick GaAs barriers. The dot density was estimated to be $\sim 4\times 10^{10}$ cm^{-2}/layer. Delta-doping layers were grown 2 nm below the QD wetting layers. The nominal doping level was adjusted such that an average doping of one electron per dot is achieved. The low-temperature photoluminescence (PL) displays emission centered at an energy of 1.17 eV with an inhomogeneous broadening of ~80 meV [full width at half maximum (FWHM)].

The low-temperature ISL absorption of the sample was measured with a Fourier-transform infrared (FTIR) spectrometer and exhibits resonances at $\hbar\omega_- = 48$ meV and $\hbar\omega_+ = 53.5$ meV for in-plane polarized light along the [−110] and [110] directions, respectively. These resonances are attributed to single-particle transitions between the QD electron ground state $|s\rangle$ and the first excited states $|p^-\rangle$ and $|p^+\rangle$.[10] The splitting of the $|p\rangle$ states is a consequence of the dot confinement potential anisotropy; the broadening of the transitions [~5 meV (FWHM)] reflects the lateral size distribution of the QDs. The average dot population was estimated from the magnitude of the ISL absorption (~25% at $T = 5$ K) and it was found that it is indeed close to 1. As the temperature is raised to $T = 300$ K, a significant decrease in ISL absorption is observed with the onset occurring at ~70 K. This decrease is attributed to thermionic emission of QD electrons into the wetting layer and the GaAs continuum.[3]

The transient FIR properties of the QDs were investigated by ultrabroadband terahertz time-domain spectroscopy,[11] which allows determining the complex dielectric function of materials by measuring not only the intensity but also the phase shift of the terahertz electromagnetic wave. In our apparatus we use a mode-locked Ti:sapphire laser that delivers 10-fs pulses centered at 780 nm wavelength (~100 nm FWHM bandwidth). Part of the laser intensity was used to generate free electron-hole pairs in the GaAs barriers and the wetting layer via interband transitions. A few-cycle terahertz electric field transient served as a probe of the field response of the nonequilibrium carrier distribution at time delay τ after photoexcitation. Alternatively, in some measurements a continuous-wave (cw) laser was used for excitation. The terahertz transient was generated by phase-matched difference mixing in a 30-μm-thick GaSe crystal. Its detection was accomplished by electro-optic sampling in a 10-μm-thick ZnTe crystal.[11] The terahertz spectrum, shown in the inset of Fig. 1(a), spans the range between ~30 and ~150 meV.

Figure 1 displays amplitude- and phase-resolved absorption data for FIR radiation, linearly polarized along the [110]

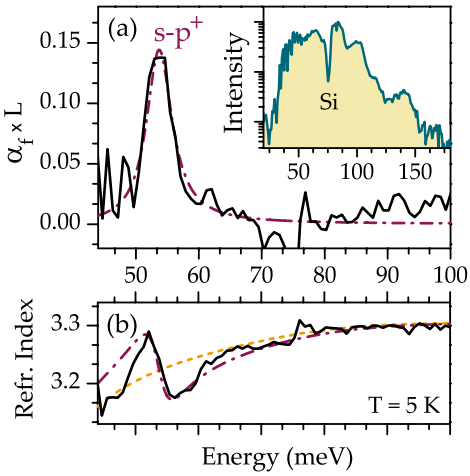

FIG. 1. (Color online) Frequency dependence of the absorption coefficient (a) and the refractive index (b) measured with terahertz pulses polarized along the [110] direction (T=5 K). The dashed line in (b) represents the variation of the GaAs matrix refractive index. The dash-dotted lines are fits according to a Lorentz model. Inset: spectrum of the ultrabroadband terahertz transient (logarithmic scale). The strong absorption at ~75 meV stems from the Si cryostat windows.

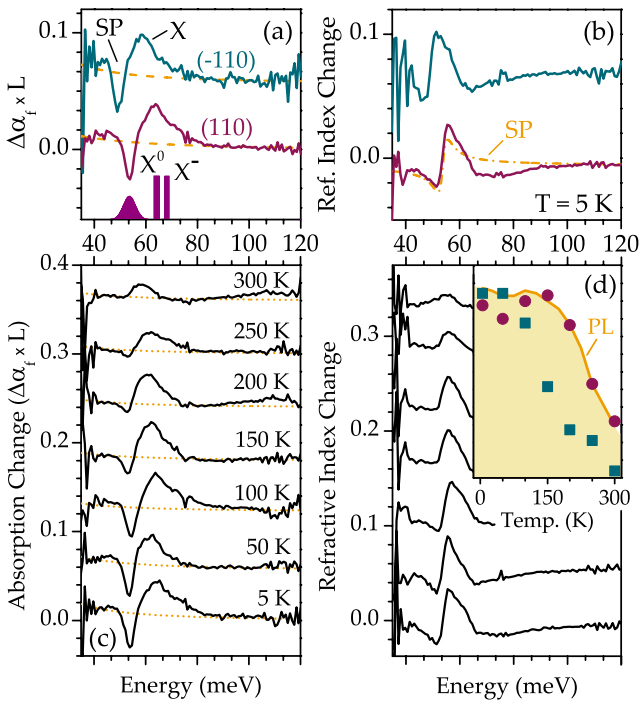

FIG. 2. (Color online) Photoinduced absorption (a) and refractive index (b) change versus frequency for 815 nm cw excitation and two different polarizations of the FIR probe. The Gaussian on the bottom of (a) represents the energetic position of the [110] ISL transition. The two bars indicate the calculated energetic positions of the [110] X^0 and X^- absorptions. The dash-dotted line in (b) shows the calculated index variation due to the SP bleaching only. (c) and (d) show temperature-dependent measurements. The dashed lines are results from a Drude model to fit the background. The curves are offset for clarity. Inset: temperature dependence of the X (circles) and SP (squares) amplitudes. The PL peak intensity is shown as a solid line.

direction of the QD sample. The data were obtained by measuring the shapes of terahertz transients after propagation through the QD sample and a GaAs reference sample. In order to account for interface effects we extracted the dielectric function through an iterative procedure.[12,13] From Fig. 1(a) we extract a peak absorption of $[1-\exp(-2\alpha_f L)] \times 100\% \sim 25\%$, in agreement with the FTIR measurement. In addition to the absorption, the variation of index of refraction was deduced from the time-domain measurement. It is shown in Fig. 1(b). Probing the $|s\rangle \rightarrow |p^-\rangle$ absorption yielded similar results.

Next, we investigated the change of the dielectric function when exciting the sample surface with a Ti:sapphire cw laser tuned to 815 nm wavelength. Photoinduced absorption [Fig. 2(a)] and refractive index [Fig. 2(b)] changes were extracted from terahertz time-domain scans recorded with and without optical excitation[12] (T=5 K, P_{ex}=300 W/cm^2). The terahertz transient was polarized either along the [−110] (upper curve) or the [110] direction (lower curve). In both cases we observe (partial) bleaching of the $|s\rangle \rightarrow |p\rangle$ single-particle transition (labeled SP) and photoinduced absorption [labeled X, ~10 meV spectral width (FWHM)] at higher energy—59 and 64 meV, respectively. In addition, a broad background is observed which is attributed to Drude absorption by free carriers which are not captured into the QDs. The Drude model provides a reasonable description of the background [see dotted lines in Fig. 2(a)]. The fact that the energetic position of X depends on the in-plane polarization of the incident light demonstrates that it originates from the dots. It might be expected that the data can be interpreted in terms of a single-particle picture, wherein electrons are captured and gradually fill the QD ground and excited states. A filled p shell would cause bleaching of the $|s\rangle \rightarrow |p\rangle$ transition and would also induce $|p\rangle \rightarrow |d\rangle$ absorption. However, we can rule this out for several reasons: (i) Spectra similar to the ones shown in Fig. 2 are observed for a wide range of excitation densities. (ii) Temperature- and (iii) time-dependent measurements of the photoinduced absorption are in contradiction to this interpretation—see discussion below. Rather, we interpret the data in terms of terahertz absorption of electrons in the presence of additional photogenerated holes (excitons) in the dots.

In order to support this interpretation we modeled the FIR absorption of excitons following Korkusinski's approach.[7] We consider neutral (X^0) as well as negatively charged (X^-) excitons.[14] It is reasonable to assume that the electronic QD single-particle wave functions φ_{nm} are well described by those of a two-dimensional harmonic oscillator, and their energies are $E^e_{nm}=\hbar\omega_e(n+m+1)$, with angular momentum $L^e=m-n$.[1] The hole single-particle states ϕ_{nm} are written analogously, where the angular momentum, however, is defined $L^h=n-m$ due to the opposite sign of the hole charge. The single-particle electron and hole wave functions are scaled by effective lengths $l_e=\sqrt{\hbar/m^*_e\omega_e}$ and $l_h=\sqrt{\hbar/m^*_h\omega_h}$, respectively. We calculate the FIR absorption of the many-particle states by finding the energy difference between the ground and excited states. The excited state configurations

which participate in the FIR absorption are those having the same total spin as the ground state and total angular momentum differing by ±1.[15] We construct the total wave function for electrons and holes for a particular configuration from the single-particle states and include then perturbatively the influence of Coulomb interactions and QD anisotropy. When building the many-particle basis set we shall limit ourselves to considering only the lowest-energy excitations. The total wave function of the neutral exciton X^0 in its ground state configuration is written as $|gs\rangle=\varphi_{00}(r_e)\phi_{00}(r_h)$. The lowest-energy electronic and hole excitations with angular momentum $L=+1$ are $|e_+\rangle=\varphi_{01}(r_e)\phi_{00}(r_h)$ and $|h_+\rangle=\varphi_{00}(r_e)\phi_{10}(r_h)$, respectively. The $L=-1$ wave functions are constructed analogously. The many-body Hamiltonian $H=H_e+H_h-V_{eh}+\delta V_e$, written in the basis of these configurations, reads

$$H=\begin{pmatrix} \hbar\omega_e+V_0/4 & \delta_e/2 & -V_0/4 & 0 \\ \delta_e/2 & \hbar\omega_e+V_0/4 & 0 & -V_0/4 \\ -V_0/4 & 0 & \hbar\omega_h+V_0/4 & 0 \\ 0 & -V_0/4 & 0 & \hbar\omega_h+V_0/4 \end{pmatrix}, \tag{1}$$

where we set the ground state energy $E_{gs}=\hbar\omega_e+\hbar\omega_h-\langle gs|V_{eh}|gs\rangle$ to zero. H_e and H_h describe the single-particle Hamiltonians, V_{eh} denotes the electron-hole Coulomb attraction, and δV_e describes the mixing of the $L=\pm1$ orbitals due to the slight anisotropy of the dots.[10] The mixing causes a splitting of the electronic p-shell energy levels by an amount δ_e. The splitting in the valence band is omitted ($\delta V_h=0$). The average oscillator frequency $\hbar\omega_e$ as well as δ_e are taken from the FTIR measurements: $\hbar\omega_e=\hbar(\omega_++\omega_-)/2=50.75$ meV; $\delta_e=\hbar(\omega_+-\omega_-)=5.5$ meV. Since in InAs QDs $m_e^*\omega_e\approx m_h^*\omega_h$, it is reasonable to assume that the electron and hole wave functions have the same lateral spatial extent,[16] i.e., $l_e\approx l_h\approx l=4.6$ nm ($m_e^*=0.07$, $m_h^*=0.112$). Under this symmetry condition we obtain $\omega_h=31.7$ meV, in agreement with the value obtained from an eight-band k·p calculation (31 meV). Furthermore, all Coulomb integrals can be evaluated analytically[17] and expressed in terms of the lowest-shell element $\langle gs|V_{eh}|gs\rangle=V_0=\sqrt{\pi/2}e^2/4\pi\varepsilon_0\varepsilon_r l=32.7$ meV. Note that the matrix elements $-\langle e_\pm|V_{eh}|h_\pm\rangle=-V_0/4$ mix configurations with same angular momentum.[7] Diagonalization of Eq. (1) yields the following positions of the absorption lines: 37.2 and 64.4 meV for light polarized along the [110] direction, and 36.5 and 59.6 meV for [−110] polarization. The low-energy transitions (37.2 and 36.5 meV) not only exhibit much weaker oscillator strengths than the high-energy excitations, but energetically also coincide with the Reststrahlen band. They are thus experimentally not observable.

A similar analysis has been performed to calculate the FIR absorption of negatively charged excitons. The ground state of the X^- corresponds to two electrons forming a singlet on the s-shell electronic orbital, and the hole occupying the s shell in the valence band. Its total (spatial) wave function is written as $|gs\rangle=\varphi_{00}(r_{e1})\varphi_{00}(r_{e2})\phi_{00}(r_h)$. Again, only four (low-energy) final state configurations are optically active and need to be considered.[7] These states are generated by promoting one electron or one hole into the $L=+1$ or $L=-1$ p shell. The $L=+1$ excited states are represented by the following antisymmetric spin singlets: $|e_+\rangle=1/\sqrt{2}[\varphi_{00}(r_{e1})\varphi_{01}(r_{e2})+\varphi_{01}(r_{e1})\varphi_{00}(r_{e2})]\phi_{00}(r_h)$ and $|h_+\rangle=\varphi_{00}(r_{e1})\varphi_{00}(r_{e2})\phi_{10}(r_h)$. The $L=-1$ wave functions are similar. The many-body Hamiltonian is written in the basis of these configurations:

$$H=\begin{pmatrix} \hbar\omega_e+V_0/4 & \delta_e/2 & -\sqrt{2}V_0/4 & 0 \\ \delta_e/2 & \hbar\omega_e+V_0/4 & 0 & -\sqrt{2}V_0/4 \\ -\sqrt{2}V_0/4 & 0 & \hbar\omega_h+V_0/2 & 0 \\ 0 & -\sqrt{2}V_0/4 & 0 & \hbar\omega_h+V_0/2 \end{pmatrix}, \tag{2}$$

and diagonalized to give the following numerical results: 41.4 and 68.3 meV for [110] polarization, and 39.9 and 64.4 meV for [−110] polarization. Thus it appears that the charged excitons absorb FIR light at slightly higher energy than the neutral excitons. We expect the photoinduced absorption peak X to consist mainly of contributions from X^0 and X^-. It becomes clear now that in our measurements X appears broadened, as it is an average of two slightly shifted absorptions. The bars in Fig. 2(a) indicate the energetic positions of the calculated X^0 and X^- [110] absorption lines, respectively. Excellent agreement with the experiment is obtained.

The exciton picture is further supported by temperature-dependent measurements, shown in Figs. 2(c) and 2(d). Different thermal behaviors are observed for the single-particle bleaching (SP) and the exciton absorption (X). The absorption amplitude of X decreases only by a factor of ~3 from low to room temperature, whereas SP vanishes almost completely. From the inset of Fig. 2(d) it becomes clear that the amplitudes of the two peaks are not correlated. Thus, we conclude that they are related to different physical processes. As the temperature increases, the doped dots get thermally depopulated, and it becomes more difficult to bleach the SP transition. The peak amplitude of X is plotted as circles in the inset of Fig. 2(d). With increasing temperature from 5 to 150 K, a slight rise of the terahertz absorption is observed. This behavior is attributed to thermalization of carriers among QDs with different sizes.[18] The decrease of absorption for $T>150$ K reveals that the dots get thermally depopulated toward the wetting layer and the GaAs continuum. It is interesting that the photoinduced signal X exhibits weaker temperature dependence than the ISL absorption of electrons only.[3] This may reflect the higher activation energy for thermal escape of excitons as compared to electrons.[19] The solid line in the inset shows the temperature dependence of the PL peak intensity from the dots ($\lambda_{ex}=815$ nm). With increasing temperature, quenching of the PL is observed.[18] The onset of quenching is consistent with that of the terahertz absorption measurement (circles), and at elevated temperatures, the PL intensity follows exactly the behavior of the absorption. The strong similarity between terahertz absorption and PL supports our previous interpretation of the data in terms of FIR absorption of excitons.

Figure 3 shows the temporal evolution of the absorption (a) and refractive index (b) change after excitation with a

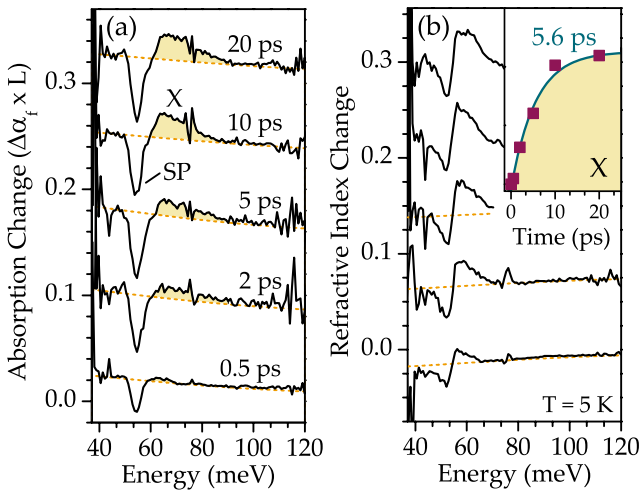

FIG. 3. (Color online) Buildup of the exciton absorption X (shaded area). Absorption coefficient (a) and refractive index change (b) versus frequency for different pump-probe delays after photoexcitation. The dashed lines result from a Drude fit of the background. The curves are offset for clarity. Inset: time dependence of the X amplitude (symbols—measurement; line—exponential fit).

10-fs interband pump pulse (P_{ex}=20 W/cm^2).[20] The Drude model provides a good description of the broad absorption background for all time delays, indicating a fast thermalization of the photoexcited carrier distribution in the GaAs barriers. The exciton absorption X rises slowly and reaches its maximum after ~20 ps. The slow rise reflects the effective capturing of holes and electrons into the QD ground state. From the absorption data we deduce a capture time of τ_c ~5.6 ps [see inset of Fig. 3(b)]. Our results are in good agreement with other measurements reported for doped InAs dots.[21,22] The maximum reached is roughly proportional to the pump intensity (exponent ~1.3) and shows a saturation behavior for $P_{ex}>100$ W/cm^2. Furthermore, at high excitation power a shortening of the rise time is observed (~3 ps at 200 W/cm^2). The interesting point is the following: One tends to believe that the FIR radiation probes the electronic $|s\rangle \rightarrow |p\rangle$ ISL transition and the temporal rise of the absorption reflects the capture of electrons into the QDs. However, since the dots are doped with electrons, the solely capture of holes would already transfer oscillator strength from the SP to the X transition. The rise of the X absorption would then reflect the capture of holes, not electrons. τ_c should thus be regarded as the time constant with which excitons form in the QDs. Let us now turn our attention to the bleaching signal SP. As can be seen from Fig. 3, SP shows an entirely different dynamics than the absorption X: 2 ps after photoexcitation it has almost reached its maximum modulation. It also exhibits a different temperature dependence (see Fig. 2). Obviously, not only the transfer of oscillator strength from single-particle to exciton transitions, but also other processes influence the bleaching. We argue that the dots are not equally populated at low temperature. A fraction of QDs is populated with one electron, others are empty, and a significant fraction of dots is doubly charged. After optical excitation, electrons get trapped rapidly into the p shell of the doubly charged dots. These carriers contribute to the fast bleaching of the absorption. On a longer time scale, holes and further electrons get trapped—we obtain excitons, singly charged excitons, and doubly charged excitons. These states contribute to the onset of the positive terahertz absorption at higher energy. The absorption is broadened since the lines are slightly shifted in energy, as discussed above. The ratio between the integrated positive absorption and the bleached absorption also provides indications on the initial population of the dots.

Our findings have important consequences for the interpretation of time-resolved measurements of carrier capture and relaxation processes in QDs. Obviously, it is not sufficient to probe the time-dependent ISL absorption at a fixed energy, but instead the dynamics of the entire absorption spectrum has to be monitored in order to really account for the trapping of different particles (electrons, holes, excitons, and charged excitons).

This work was supported by the ECNoE program SANDiE and the Austrian Fonds zur Förderung der Wissenschaftlichen Forschung (SFB-ADLIS, SFB-IRON).

*thomas.mueller@tuwien.ac.at

[1] See, for example, *Single Quantum Dots*, edited by P. Michler (Springer, Berlin, 2003), and references therein.
[2] S. Sauvage, P. Boucaud, R. P. S. M. Lobo, F. Bras, G. Fishman, R. Prazeres, F. Glotin, J. M. Ortega, and J. M. Gerard, Phys. Rev. Lett. **88**, 177402 (2002).
[3] F. Bras, P. Boucaud, S. Sauvage, G. Fishman, and J.-M. Gérard, Appl. Phys. Lett. **80**, 4620 (2002).
[4] E. A. Zibik, L. R. Wilson, R. P. Green, G. Bastard, R. Ferreira, P. J. Phillips, D. A. Carder, J-P. R. Wells, J. W. Cockburn, M. S. Skolnick, M. J. Steer, and M. Hopkinson, Phys. Rev. B **70**, 161305(R) (2004).
[5] H. Drexler, D. Leonard, W. Hansen, J. P. Kotthaus, and P. M. Petroff, Phys. Rev. Lett. **73**, 2252 (1994).
[6] M. Fricke, A. Lorke, J. P. Kotthaus, G. Medeiros-Ribeiro, and P. M. Petroff, Europhys. Lett. **36**, 197 (1996).
[7] M. Korkusinski, Phys. Rev. B **74**, 075317 (2006).
[8] F. Wang, J. Shan, M. A. Islam, I. P. Herman, M. Bonn, and T. F. Heinz, Nat. Mater. **5**, 861 (2006).
[9] E. Hendry, M. Koeberg, F. Wang, H. Zhang, C. de Mello Donegá, D. Vanmaekelbergh, and M. Bonn, Phys. Rev. Lett. **96**, 057408 (2006).
[10] S. Hameau, J. N. Isaia, Y. Guldner, E. Deleporte, O. Verzelen, R. Ferreira, G. Bastard, J. Zeman, and J. M. Gerard, Phys. Rev. B **65**, 085316 (2002).
[11] R. Huber, A. Brodschelm, F. Tauser, and A. Leitenstorfer, Appl. Phys. Lett. **76**, 3191 (2000).
[12] M. Schall and P. U. Jepsen, Opt. Lett. **25**, 13 (2000).

[13] The 80 dot layers were treated as a homogeneous absorbing medium with thickness $L=80\times 50$ nm$=4$ μm.

[14] For simplicity we do not consider multiply charged excitons here, although we expect them to contribute to the FIR absorption as well (especially X^{2-}).

[15] A. Wojs and P. Hawrylak, Phys. Rev. B **53**, 10841 (1996).

[16] P. Hawrylak, Phys. Rev. B **60**, 5597 (1999).

[17] R. J. Warburton, B. T. Miller, C. S. Dürr, C. Bödefeld, K. Karrai, J. P. Kotthaus, B. Medeiros-Ribeiro, P. M. Petroff, and S. Huant, Phys. Rev. B **58**, 16221 (1998).

[18] P. Dawson, O. Rubel, S. D. Baranovskii, K. Pierz, P. Thomas, and E. O. Göbel, Phys. Rev. B **72**, 235301 (2005).

[19] H. Pettersson, L Landin, R. Liu, W. Seifert, M.-E. Pistol, and L. Samuelson, Appl. Phys. Lett. **85**, 5046 (2004).

[20] When comparing cw with pulsed excitation intensities one has to take the ratio between the repetition time of the laser pulses τ_R ($\sim$15 ns) and the average carrier lifetime τ_L ($\sim$1 ns) into account. $P_{\mathrm{ex}}=20$ W/cm^2 in pulsed mode operation corresponds to $\sim$300 W/cm^2 under cw excitation.

[21] K. Gündoğdu, K. C. Hall, Thomas F. Boggess, D. G. Deppe, and O. B. Shchekin, Appl. Phys. Lett. **85**, 4570 (2004).

[22] J. Siegert, S. Marcinkevicius, and Q. C. Zhao, Phys. Rev. B **72**, 085316 (2005).